CHAPTER 7

DSMC Chemistry Modeling

7.1 Overview

Completion of the nominal simulations in Chapter 4, preliminary sensitivity analyses in Chapter 5, and Saturn simulations in Chapter 6 demonstrated various ways in which the results of the CHIPS simulations of ionizing, hypersonic shock waves are affected by chemical reactions. Information gained from these results can now be put to use in the improvement of several CHIPS models. First, the significant difference in the two nominal simulations and sensitivity analysis studies due to the inclusion of an electronic excitation model needs further examination. The effect of electronically excited states on the ionization rate must be understood due to the high ranking of ionization reactions in the sensitivity analysis results. In the preliminary conclusions of Chapter 5, it was also postulated that the backward reaction model plays an important role in simulating several reactions, such as electron capture reactions. The importance of backward reaction modeling was again highlighted in the Saturn entry simulations when the free electron number density was greater than the expected equilibrium concentration. One issue with the current backward reaction model is that the chemical reaction set is missing several backward reaction rates that are likely to prevent the correct equilibrium composition from forming. All these concerns involving the CHIPS chemistry model are investigated in the current chapter.

7.2 Arrhenius Chemistry

Before the chemistry models used in DSMC can be analyzed, a brief overview of Arrhenius chemistry is required. Let us consider a reaction with N_r reactants that results in N_p products,

$$\sum_{i=1}^{N_r}(\alpha_i X_i) \rightleftharpoons \sum_{j=1}^{N_p}(\beta_j X_j) \qquad [7.1]$$

$$\alpha_r = \sum_{i=1}^{N_r}\alpha_i - 1 \qquad [7.2]$$

$$\beta_p = \sum_{j=1}^{N_p}\beta_j - 1 \qquad [7.3]$$

where X_i is any reacting molecular species, α_i and β_j are stochiometric constants, and the forward reaction in Eqn. 7.1 proceeds from left to right. The forward reaction rate, k_f, is represented in modified Arrhenius form by the equation

$$k_f(T) = \Lambda_f T^{\eta_f} exp\left(-{E_{a_f}}/{k_B T}\right) \qquad \left[\frac{1}{s}\left(\frac{cm^3}{mol}\right)^{\alpha_r}\right] \qquad [7.4]$$

where Λ_f is the pre-exponential constant, η_f is the temperature exponent, and E_{a_f} is the activation energy. The activation energy is the minimum energy required for the reaction to occur and is typically fairly well known for a specific reaction. The constants, Λ_f and η_f, are parameters that are adjusted to fit experimental or calculated forward reaction rates as a function of temperature. It is not uncommon to find differing values of these constants in the literature. The equilibrium constant, K_{eq}, is defined as

$$K_{eq}(T) = \frac{k_f(T)}{k_b(T)} \tag{7.5}$$

where k_b is the backward reaction rate. The equilibrium constant is defined such that detailed balance, or more specifically, the law of mass action is satisfied [75]. This allows the equilibrium constant to be represented as

$$\begin{aligned} K_{eq}(T) &= \frac{\prod_j^{N_p} (n_j)^{\beta_j}}{\prod_i^{N_r} (n_i)^{\alpha_i}} \\ &= \frac{\prod_j^{N_p} (Q_j)^{\beta_j}}{\prod_i^{N_r} (Q_i)^{\alpha_i}} V^{(\alpha_r - \beta_p)} exp\left(-\Delta H^\circ / k_B T\right) \quad \left[\left(\frac{mol}{cm^3}\right)^{(\beta_p - \alpha_r)}\right] \end{aligned} \tag{7.6}$$

with n_i and Q_i defined as the number density and total partition function of the current species, ΔH° as the enthalpy of the reaction from reference temperature 298.15 K, and V as the volume. Typically, the equilibrium constant is determined from high order partition functions or ab initio calculations and then the backward reaction rate is calculated by rearranging Eqn. 7.5.

7.3 Total Collision Energy Chemistry Model

Since DSMC is a particle method where chemistry must be applied on a per collision basis, the modified Arrhenius reaction rate equation cannot be used in its current form. Instead, methods have been proposed to utilize the properties of the colliding particles in order to produce the Arrhenius rate. The most widely used method for performing forward reactions with Arrhenius rate chemistry in DSMC is the Total Collision Energy (TCE) model [3][15], briefly discussed in Section 2.3.2. Other common

chemistry methods exist, such as the quantum-kinetic (Q-K) model [35] or the use of molecular dynamics/quasi-classical trajectory (MD/QCT) calculations [76], to perform chemistry in DSMC, but they do not apply Arrhenius rate equations and will not be discussed here.

When two particles are selected to collide in a chemically active DSMC simulation, a probability for each possible reaction must be determined. In the TCE model, the reaction probability is calculated from the energy contained in the colliding particles. This includes the relative translational energy of the colliding particles and the contributing internal energy of each individual particle. Once the reaction probabilities are calculated, they are each compared to a previously drawn random number to determine if a reaction takes place. If a reaction is selected to occur, the reaction products are created and the total relative translational and internal energies of the reactants, less the enthalpy of reaction, $\Delta H°$, are redistributed to the products using the Borgnakke-Larsen model [25]. While this seems straightforward, there have recently been misunderstandings with the assumptions and limitations of the TCE model that will be discussed in the following sections.

7.3.1 TCE Model Derivation

First, a brief analysis of the TCE model's derivation is required. In Bird's 1994 book [3], the derivation of the TCE model begins with the distribution functions for the relative translational and internal energy of the colliding particles (pg. 104-5, 126). While this is a valid starting point, the derivation of the distribution function for internal energy must be considered to understand the underlying assumptions in the TCE model. The subsequent summary follows Hinshelwood's derivation of the distribution function for

internal energy [77]. Hinshelwood begins by defining a momentum coordinate, p, and its corresponding energy, ε, for some motion in a coordinate, x.

$$p = mx, \quad \varepsilon = \frac{1}{2}mx^2 \tag{7.7}$$

Every different coordinate, x, describes a separate degree of freedom such as a directional velocity (translational), angular momentum (rotational), etc. This representation of momentum and energy follows from classical mechanics where each degree of freedom contributes a single quadratic ("square") term to the energy. It is important to note that, from the equipartition theorem, each individual degree of freedom that is quadratic in energy contributes equally to the total energy in thermal equilibrium. It can be shown that this quantity is

$$\bar{\varepsilon} = \frac{1}{2}k_B T \tag{7.8}$$

where $\bar{\varepsilon}$ is the average energy that the single degree of freedom possesses at equilibrium.

Now consider a series of quantized energy states $\varepsilon_i = \varepsilon_1, \varepsilon_2, \ldots, \varepsilon_M$ where the probability of a particle being in state j is defined by the Boltzmann distribution as

$$\frac{N_j}{N} = \frac{exp\left(-{\varepsilon_j}/{k_B T}\right)}{\sum_{i=1}^{M} exp\left(-{\varepsilon_i}/{k_B T}\right)} \tag{7.9}$$

with N_j being the number of particles in state j. This fraction can be converted from the quantum to the classical theory by following Hinshelwood and the number of particles, dN, with momentum between p and $p + dp$ is found to be

$$\frac{dN}{N} = \frac{\varepsilon^{-\frac{1}{2}} exp\left(-{}^{\varepsilon}/_{k_B T}\right) d\varepsilon}{\sqrt{\pi k_B T}} \qquad [7.10]$$

which is true regardless of the type of energy, translational or internal. If a particle with ζ degrees of freedom is now considered, there are ζ different quadratic terms that contribute to the fraction of molecules where the total energy, E, is between E and $E + dE$. By combining and integrating each term, this fraction becomes

$$\frac{dN}{N} = \frac{1}{(\pi k_B T)^{\frac{1}{2}\zeta}} \int_0^E \int_0^E \dots \varepsilon_1^{-\frac{1}{2}} exp\left(-{}^{\varepsilon_1}/_{k_B T}\right) d\varepsilon_1 \times \varepsilon_2^{-\frac{1}{2}} exp\left(-{}^{\varepsilon_2}/_{k_B T}\right) d\varepsilon_2 \dots \\ \dots [E - (\varepsilon_1 + \varepsilon_2 \dots)]^{-\frac{1}{2}} exp\left(-{}^{[E - (\varepsilon_1 + \varepsilon_2 \dots)]}/_{k_B T}\right) dE \qquad [7.11]$$

where the energy in the final term, ε_ζ, is replaced by rearranging

$$E = \varepsilon_1 + \varepsilon_2 + \cdots + \varepsilon_\zeta \qquad [7.12]$$

After integrating Eqn. 7.11, the distribution of E is found to be

$$f_{\left(E/k_BT\right)} = \frac{\left(E/k_BT\right)^{\frac{\zeta}{2}-1} exp\left(-E/k_BT\right)}{\Gamma\left(\frac{\zeta}{2}\right)} \quad [7.13]$$

which has been normalized by k_BT. This is the distribution function for the internal energy in a molecule with ζ degrees of freedom and is the starting point in Bird's 1994 book [3].

Following Bird's derivation, the reaction cross-section, σ_R, for two colliding particles A, B with a total collision energy, E_c, is assumed to take the form

$$\sigma_R = \begin{cases} 0 & if\ E_c < E_a \\ \sigma_T C_1 (E_c - E_a)^{C_2} (1 - E_a/E_c)^{\zeta_I + 3/2 - \omega_{A,B}} & if\ E_c > E_a \end{cases} \quad [7.14]$$

where C_1 and C_2 are constants to be determined, σ_T is the total collision cross-section, and

$$\zeta_I = \sum_{i=1}^{N_{\zeta_A} + N_{\zeta_B}} \frac{\zeta_i}{2} \quad [7.15]$$

which is the total contribution of the internal degrees of freedom of each particle. In Eqn. 7.15, N_{ζ_A} and N_{ζ_B} are the number of contributing internal degrees of freedom from particles A and B. Note that calling ζ_I the "average degrees of freedom" is a common misconception in the DSMC community because the two in the denominator of Eqn. 7.15 originates from the assumption that ε is a square term (Eqn. 7.7), not from averaging the degrees of freedom between colliding particles A and B. Also, the total collision energy

(Eqn. 7.16) is determined from the sum of the relative translational energy of the colliding particles, E_{tr}, and the internal energy of each contributing internal mode, E_{int}.

$$E_c = E_{tr} + \sum_{i=1}^{N_{\zeta_A}+N_{\zeta_B}} E_{int_i} \quad [7.16]$$

After determining the constants in Eqn. 7.14 by considering the Variable Hard Sphere (VHS) model [15] collision frequency and comparing with the modified Arrhenius equation (Eqn. 7.4), the reaction probability for binary collisions with $E_c > E_a$ is found to be

$$P_{react} = \frac{\sigma_R}{\sigma_T}$$

$$= \frac{\sqrt{\pi}\left(1+\delta_{A,B}\right)\Lambda T_{ref_{A,B}}^{\eta}}{2\pi d_{ref_{A,B}}^2 \left(k_B T_{ref_{A,B}}\right)^{\eta-1+\omega_{A,B}}} \frac{\Gamma\left(\zeta_I + \frac{5}{2} - \omega_{A,B}\right)}{\Gamma\left(\zeta_I + \eta + \frac{3}{2}\right)} \sqrt{\frac{m_r}{2k_B T_{ref_{A,B}}}} \frac{\left(E_c - E_a\right)^{\eta+\zeta_I+\frac{1}{2}}}{E_c^{\zeta_I+\frac{3}{2}-\omega_{A,B}}} \quad [7.17]$$

In Eqn. 7.17, the VHS parameters for the colliding particles (A, B) are d_{ref}, T_{ref}, and ω. Also, $\delta_{A,B}$ is one when $A = B$ and zero otherwise. This is the final form of the TCE model and is used to calculate the reaction probability for each possible reaction that a pair of colliding particles can undergo.

7.3.2 Limitations Due to Model Requirements

In the TCE model, the reaction probability calculated from Eqn. 7.17 is solely dependent on the properties of the colliding particles being considered. While this is advantageous for simulating a non-equilibrium flow, there are various limitations that

must be considered when utilizing the TCE model. Analysis of the relationships between the contributing internal degrees of freedom, ζ_I, the VHS temperature-viscosity exponent, $\omega_{A,B}$, and the Arrhenius temperature exponent, η in Eqn. 7.17 identifies some of these limitations. In order for Eqn. 7.17 to produce the expected or, in some cases, realistic trends, these parameters must satisfy various constraints. First, the reaction probability must tend to zero as E_c approaches E_a since a nonzero reaction probability at the activation energy is unphysical. This leads to the requirement that the Arrhenius temperature exponent must satisfy $\eta > -\zeta_I - 1/2$ and represents the lower limit for η. If this requirement is not met, the reaction probability approaches infinity when $E_c = E_a$ and is clearly unphysical. The upper limit of η is not as easily defined and previous publications have identified the upper limit from Eqn. 7.17 to be $\eta < \omega_{A,B} - 1$ [3][36]. This limit is intended to be set so that the reaction probability approaches zero as E_c approaches infinity. Analysis of Eqn. 7.14 yields a different result for this upper limit. Since it is desired that $\sigma_R \to 0$ when $E_c \to \infty$, the value of C_2 must be negative so that the term $(E_c - E_a)^{C_2}$ appears in the denominator. In the original derivation of Eqn. 7.17, it was found that $C_2 = \eta - 1 + \omega_{A,B}$ and leads to the conclusion that the upper limit is actually $\eta < 1 - \omega_{A,B}$. If η is greater than this limit, the reaction rate increases monotonically towards infinity as the collision energy increases instead of decreasing back to zero. In summary, the Arrhenius temperature exponent must satisfy

$$-\zeta_I - 1/2 < \eta < 1 - \omega_{A,B} \qquad [7.18]$$

which represents the hard limits of the η values. If these constraints are met, the reaction probability will be zero when $E_c = E_a$, increase to some maximum probability as E_c

increases, and then decrease back to zero as E_c approaches infinity. An example of the expected trend is shown by the $\eta = -1.5$ case in Fig. 7.1 for the dissociation reaction $O_2 + N_2 \rightleftharpoons O + O + N_2$ which represents the reaction probability as a function of collision energy for the published value of the Arrhenius temperature exponent. Only the rotational modes are considered in this case with the parameters used in this calculation listed in Tables 7.1 and 7.2 [3][44][48].

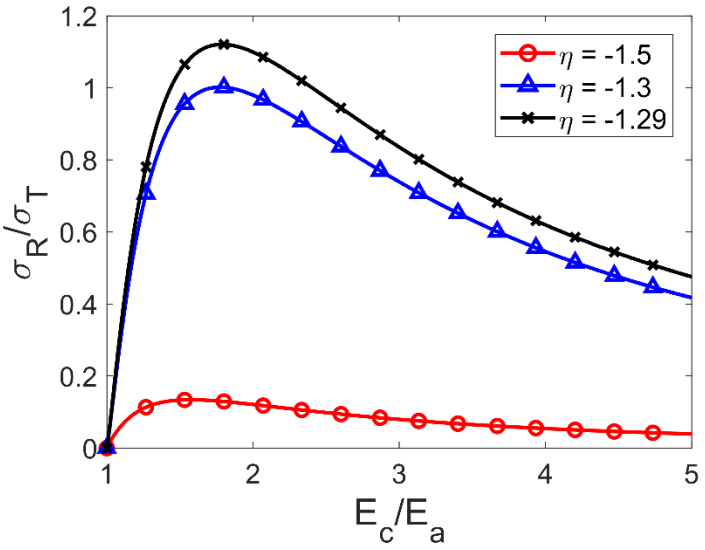

Figure 7.1 TCE reaction probability as function of the collision energy for various values of η in the O_2 dissociation reaction, $O_2 + N_2 \rightleftharpoons O + O + N_2$.

Table 7.1 Arrhenius rate reactions and equilibrium constants used in this chapter.

Reaction	Forward Arrhenius Rate, k_f [m^3/molec-s]			Backward Arrhenius Rate, k_b [m^3/molec-s]	
$O_2 + N_2 \rightleftharpoons O + O + N_2$	$3.321 \times 10^{-9} T^{-1.5} \exp(-59400/T)$				
$O + N_2 \rightleftharpoons N + NO$	$1.069 \times 10^{-12} T^{-1.0} \exp(-37500/T)$			$4.059 \times 10^{-12} T^{-1.359}$	
Park's equilibrium constant, K_{eq} [47]	A_1	A_2	A_3	A_4	A_5
$O_2 + N_2 \rightleftharpoons O + O + N_2$	0.967940	0.891310	0.729100	-3.955500	0.006488

Table 7.2 Species model parameters used in this chapter.

Species i	N_2	N	O_2	O	NO
VHS reference diameter, d_{ref_i} [m]	4.17×10^{-10}	3.00×10^{-10}	4.07×10^{-10}	3.00×10^{-10}	4.20×10^{-10}
VHS temperature exponent, ω_i	0.74	0.8	0.77	0.8	0.79
Characteristic rotational temperature, θ_{rot} [K]	2.88	–	2.07	–	2.44
Characteristic vibrational temperature, θ_{vib} [K]	3390	–	2270	–	2740
Electronic energy levels	Ref. [48]	–	Ref. [48]	–	Ref. [48]

While it seems like the identification of the correct upper limit extends the range of possible η values compared to previous publications, in some cases approaching this limit may be detrimental to reproducing the correct Arrhenius rate. A parametric study where η was varied over the range of Eqn. 7.18 showed that, for some reactions, Eqn. 7.17 produces maximum reaction probabilities greater than one even if Eqn. 7.18 is satisfied. This can occur beginning at some value of η and extends until the previously

determined upper limit is reached. Probabilities greater than one cannot be accounted for in the current form of the TCE model and will result in discrepancies between the actual and simulated Arrhenius rate. Although probabilities greater than one are unphysical, they may be acceptable in certain collision energy ranges with minor adverse effects on the simulated Arrhenius rate. For example, consider the previously mentioned O_2 dissociation reaction. The upper limit for this reaction, using the parameters listed in Tables 7.1 and 7.2 and according to Eqn. 7.18, is $\eta = 0.245$, but Fig. 7.1 shows that the reaction probability will reach values greater than one when $\eta \gtrsim -1.3$. Now consider the case in Fig. 7.1 where $\eta = -1.29$. The reaction probability is realistic for $E_c < 1.4E_a$, but the probability is greater than one from 1.4 to $2.5E_a$. The region where the reaction probability is greater than one is concerning because the appropriate number of reactions will not be modeled. But, this should have a negligible effect on the simulated Arrhenius rate since a reaction this energetic is rare and it is unlikely, for most simulated scenarios, that a highly energized molecule would survive previous collisions without dissociating. If an even larger value of η is used, more of the probability curve will be larger than one and, at some point, effects on the simulated reaction rate will be felt. Unfortunately, this means that in addition to satisfying Eqn. 7.18, each reaction must be individually considered to determine if the reaction probability is greater than one for substantial portions of the collision energy range significant to the intended DSMC application. The effect on the Arrhenius rate can be studied by initializing a single DSMC cell in equilibrium at some temperature of interest, counting the number of accepted reactions (without performing the reactions/collisions), and comparing the simulated DSMC reaction rate to the expected Arrhenius rate.

7.3.3 Solutions for Satisfying Model Requirements

Arrhenius reaction rate values are typically compiled from published curve fits of ab initio or experimental results. As might be expected, these Arrhenius rates are published without regard for the limitations of the TCE model, so it is not unusual to encounter Arrhenius temperature exponent values that violate the constraints of the TCE model. The standard approach to using these reaction rates with TCE is to refit the Arrhenius parameters, Λ and η, to the original Arrhenius rate over the temperature range of interest, while constraining η to values compatible with the TCE model. While this avoids introducing errors through the TCE model, the simulated reaction rate may no longer be as accurate as the original Arrhenius rate. As an alternative to refitting the Arrhenius rate equation for certain cases, the VHS parameters could be refit so that $\omega_{A,B}$ is small enough to allow for a larger η value. While the effects of changing $\omega_{A,B}$ are much more difficult to predict, sensitivity analysis results for a high temperature reacting heat bath DSMC simulation have shown that results may be much more sensitive to reaction rate parameters than VHS parameters [78]. This is most likely due the relatively small variation of the VHS cross-section with temperature as high temperatures are reached [56].

While the approach of refitting parameters provides a simple solution, another method is available to remedy a subset of the issues with the Arrhenius temperature exponent. The derivation of the TCE model (Eqn. 7.17) assumes that the total collision cross-section, σ_T, is equivalent to the VHS cross-section, σ_{VHS} [3]. This approximation is valid for a pair of colliding particles as long as the total reaction probability of all the possible reactions for that pair is small, meaning that the reaction cross-section, σ_R, is much less than σ_{VHS}. This is typically true at low temperatures, but at high temperatures where dissociation and ionization are likely, the reaction cross-section can become large.

The reaction cross-section can even become greater than σ_{VHS} which will result in reaction probabilities greater than one as shown in Fig. 7.1. As previously discussed, reaction probabilities greater than one will result in an incorrect simulated Arrhenius rate. To calculate the appropriate total cross-section and avoid reaction probabilities greater than one, Strand and Goldstein proposed the modification

$$\sigma_T = \sigma_{VHS}\left(1 + \sum_{i=1}^{N_R}\left(\frac{\sigma_R}{\sigma_{VHS}}\right)_i\right) \quad [7.19]$$

where N_R is the number of possible reactions for the selected reaction pair and $(\sigma_R/\sigma_{VHS})_i$ is the reaction probability calculated from Eqn. 7.17 for each reaction, i [31]. The reaction probability for each reaction is now

$$P_{react_i} = \frac{\sigma_{VHS}}{\sigma_T}\left(\frac{\sigma_R}{\sigma_{VHS}}\right)_i \quad [7.20]$$

and the new total cross-section is also used to find the product of the total cross-section and the relative speed, $\sigma_T c_r$, which is compared to the maximum, $(\sigma_T c_r)_{max}$, to determine if a potential collision occurs. This method guarantees that the total reaction probability will not surpass one. It addresses the case where $\eta < 1 - \omega_{A,B}$, but the reaction probability is greater than one, essentially extending the limits of η to its true restrictions identified in Eqn. 7.18. One downside of including the reaction cross-section in the total cross-section is that the reaction probabilities must be calculated for each *potential* collision before it is accepted, thereby adding computational expense. Without this method, reaction probabilities were only calculated for *accepted* collisions. The other

downside is that $(\sigma_T c_r)_{max}$ can become prohibitively large. As presented by Bird [3][35], $(\sigma_T c_r)_{max}$ is used to calculate the number of potential collisions to consider at each timestep. For large values, many potential collisions must be considered. This can quickly cause a simulation to become intractable due to the sheer number of potential collisions that must be considered. An appropriate compromise for this issue is to limit Eqn. 7.17 for an individual reaction probability by selecting a maximum value, such as $P_{react_i} = 1$ which represents the case where $\sigma_{R_i} = \sigma_{VHS}$. This approach is taken in the CHIPS code and allows for improvement to the reaction modeling, but reduces the computational hit incurred by extreme values of the reaction probability.

7.3.4 Limitations Due to Model Assumptions

In addition to limitations on the TCE model parameters, the derivation of the TCE model has underlying assumptions that must be met. The derivation of the internal energy distribution (Eqn. 7.13) by Hinshelwood assumes that each degree of freedom depends quadratically on its coordinate [77]. The equipartition theorem then states that each quadratic degree of freedom contributes to an average energy of $1/2k_BT$ (Eqn. 7.8). The Borgnakke-Larsen model [25] also originates from the same internal energy distribution function and the effects of its underlying assumptions on the model have been analyzed in previous publications [79][80][81]. While much effort has been spent on the Borgnakke-Larsen model, the limitations of the TCE model due to the assumptions inherent to Eqn. 7.13 have been largely overlooked. When using the TCE model, the following restrictions must be considered.

First, the quadratic corollary to the equipartition theorem states that each degree of freedom used in the TCE model must correspond to a square term representing an average energy of $1/2k_BT$. While classical statistical mechanics restricts the degrees of

freedom used in Eqn. 7.13 to integer values [75][82], non-integer values can potentially be used as long as they satisfy the previous statement by returning the equivalent fraction of the average energy. As an example, consider the modeling of continuous rotational energy in a standard DSMC simulation. When either using the Borgnakke-Larsen model [25] to redistribute internal energy after a collision or initializing a particle entering the simulation, the internal energy is randomly selected from Eqn. 7.13 for a given temperature. Hypothetically, if the molecular species being assigned energy has a non-integer value for the rotational degrees of freedom, such as $\zeta_{rot} = 2.5$, the correct internal energy distribution and average energy of $2.5 \times 1/2k_BT$ will be produced from Eqn. 7.13. In turn, the non-integer degrees of freedom will have no effect on the reproduction of the correct Arrhenius rate by the TCE model. However, the TCE model will fail to reproduce the Arrhenius rate if the degrees of freedom and average internal energy do not match.

The second assumption contained within the equipartition theorem is that equipartition is only valid for classical statistical mechanics which requires that energy distributions are continuous. In DSMC simulations, rotational energy is typically modeled as continuous since most simulations are performed for temperatures where the rotational modes are fully excited. On the other hand, the vibrational modes are not yet fully excited for the temperatures modeled in most DSMC scenarios. It is common for DSMC simulations to be completed with quantum models for electronic and vibrational modes, such as the quantum simple harmonic oscillator (SHO) for vibration. If internal energy for certain modes are modeled discretely, these modes cannot contribute to the total collision energy used to calculate the reaction probability in Eqn. 7.17 without introducing some degree of error into the simulated reaction rate.

Figure 7.2 demonstrates the resulting error when including quantum internal energy in the TCE calculation. In Fig. 7.2, the same dissociation reaction as investigated previously (Tables 7.1 and 7.2) is considered, but this time both rotation and vibration are included in TCE where the vibrational modes are modeled with the discrete SHO. To obtain the Arrhenius rate simulated by DSMC, a single cell is filled with two million particles per species where the particles are initialized in equilibrium at the temperature of interest. During a timestep, the reaction probability is calculated for particles selected to collide, but collisions are never carried out. Instead, the number of accepted reactions is counted. Two timesteps are completed per simulation where the purpose of the first timestep is to obtain the correct total cross-section so that the appropriate number of potential collisions are considered. In the second timestep, the number of reactions are counted and this result is ensemble averaged over 16 instances of this simulation to obtain an accurate simulated Arrhenius rate. When comparing the DSMC results (Δ symbols) with the exact Arrhenius rate, a slight overshoot in the simulated reaction rate is observed at low temperatures. This error occurs because the discrete spacing in vibrational levels is important when the temperature is on the order of the characteristic vibrational temperature or lower. The value of the effective vibrational degrees of freedom is calculated as

$$\zeta_{vib} = \frac{2\theta_{vib}}{T_{vib}(e^{\theta_{vib}/T_{vib}} - 1)} \qquad [7.21]$$

where T_{vib} is the vibrational temperature and θ_{vib} is the characteristic vibrational temperature of the molecule. The SHO, and therefore, Eqn. 7.21 approaches the classical limit as the temperature becomes much larger than the characteristic vibrational

temperature. This causes the difference between the simulated and exact rate to decrease with increasing temperature. While the effects on the simulated reaction rate for this reaction are relatively small, these effects become more pronounced as the characteristic temperature or a molecule's vibrational complexity increases. This effect has been documented in a previous publication by Gimelshein, et al. where the simulated rate for a CO_2-CO_2 reaction is twice as fast as the expected rate [83]. While Gimelshein, et al. correctly pointed out that discrete representations of internal energy cannot be used in the TCE model, this was not attributed to the underlying assumptions of classical mechanics in the TCE model's derivation.

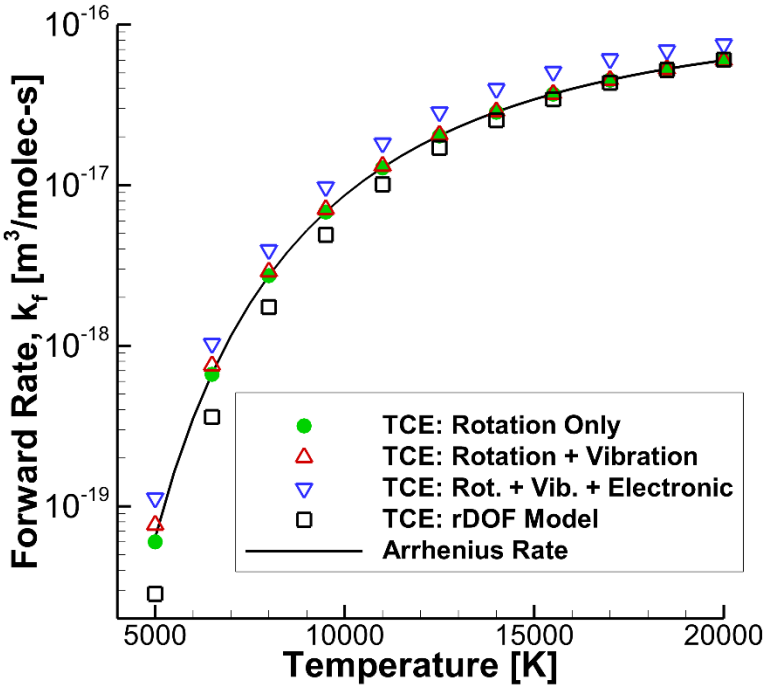

Figure 7.2 Comparison of the exact forward reaction rate for $O_2 + N_2 \rightleftharpoons O + O + N_2$ with DSMC using the TCE model with various internal mode contributions and with the rDOF model.

In the same publication, Gimelshein, et al. suggests a curve fitting method to adjust the Arrhenius parameters, Λ and η, so that discrete models can contribute to the total collision energy. This method has the distinct advantage of including the contributions of internal energy from all participating internal modes. In some cases, the energy contribution from the vibrational or electronic modes is arguably the most important for determining the reaction probability. For example, dissociation reactions rely heavily on the vibrationally excited state of the dissociating molecule and chemical models have been developed to address this dependence such as the Vibrationally Favored Dissociation model [36][84], although this model may suffer from the same discrete modeling issue as TCE. Since the curve fitting method addresses the errors from both discrete energy distributions and the resulting non-quadratic degrees of freedom, this may appropriately correct the TCE reaction probability. It is unclear whether this method has any unintended effects on non-equilibrium modeling, but it is difficult to obtain non-equilibrium cross-sections for comparison.

In addition to satisfying the equipartition theorem and being continuous, internal energy distributions used in the TCE model must follow the form of Eqn. 7.13. A somewhat common, yet unpublished, method that will be designated the reaction degrees of freedom model (rDOF) has been propagated through the DSMC community. The intention of the rDOF model is to correct the total collision energy by only including the internal energy modes that contribute to the specific reaction rate. In theory, this approach has the advantage of improving the realism for some reactions since not all available degrees of freedom may contribute to the reaction rate in a real particle collision [75]. To apply this theory, Eqn. 7.16 was modified such that

$$E_c = E_{tr} + \frac{\zeta_{react}}{\zeta_I} \sum_{i=1}^{N_{\zeta_A}+N_{\zeta_B}} E_{int_i} \qquad [7.22]$$

where ζ_{react} is the contributing degrees of freedom for the specific reaction. In addition, Eqn. 7.17 is calculated from ζ_{react} instead of using ζ_I from Eqn. 7.15. This approach seems to be allowed because the purpose of multiplying the contributing internal energy by the ratio of the degrees of freedom is to effectively scale the average energy for ζ_{react} and, therefore, would satisfy the equipartition theorem. In practice however, the rDOF model fails since the direct scaling of the internal energy for a selected reaction degrees of freedom value does not produce the correct internal energy distribution that is expected for those degrees of freedom. This failure occurs because the scaling is applied to the internal energy of the particles participating in individual collisions. In a DSMC simulation, the internal energy of the individual particles represents a collection of values randomly selected from equilibrium internal energy distribution functions (Eqn. 7.13) for each classical degree of freedom. To change the degrees of freedom represented by a simulated species, the particles must be reinitialized using the new degrees of freedom. For this reason, the scaled collision energy in the rDOF model produces the incorrect Arrhenius rate when used in the TCE model because the incorrect number of collisions are accepted for reaction. This occurs even though the TCE model is calculating the "correct" reaction probability for the scaled collision energy and degrees of freedom values.

In order to demonstrate the errors produced by the rDOF model, consider the same O_2 dissociation reaction as the previous section (Tables 7.1 and 7.2). Only the rotational modes are considered so that $\zeta_I = 2$ and an assumed reaction degrees of

freedom is set to $\zeta_{react} = 1$. Figure 7.3 shows the internal energy distributions calculated from Eqn. 7.13 for the original TCE case $\zeta = 2 \times \zeta_I = 4$ and the rDOF case $\zeta = 2 \times \zeta_{react} = 2$. To calculate the third line, representing the rDOF model, the rotational energy for a large number of particles was selected from the internal energy distribution for $\zeta = 4$. The rotational energy of each particle was then scaled following the second term on the right-hand side of Eqn. 7.22 where $\zeta_I = 2$ and $\zeta_{react} = 1$. The resulting internal energy distribution is plotted in Fig. 7.3 by the line with the ∇ symbols. This line would coincide with the $\zeta = 2$ case if the rDOF method were able to correctly modify the internal energy. Even though these lines do not match, they both will result in an average internal energy of $k_B T$ showing that the rDOF method satisfies equipartition. The resulting errors in the simulated Arrhenius rate occur because the rDOF model considers too many or too few reactions when compared to the correct distribution. Using this same example, Fig. 7.2 compares the forward rate simulated by the rDOF model in DSMC to the exact rate calculated from the Arrhenius equation in Table 7.1. Again, only the rotational modes are considered in the rDOF model. While it may seem that the rDOF model predicts the correct rate at high temperatures, this is not true for every reaction. The effect of ζ_{react} largely depends on its relationship to ζ_I, the Arrhenius parameters for the reaction, and the species involved in the reaction. In some cases, the effect of ζ_{react} is more pronounced at high temperatures and can even overpredict the reaction rate. While the simulation of the O_2 + N_2 reaction with the rDOF model shown in Fig. 7.2 still satisfies the TCE limitations set in Eqn. 7.18, this may not be the case for every reaction and would lead to further discrepancies between the simulated and exact rates.

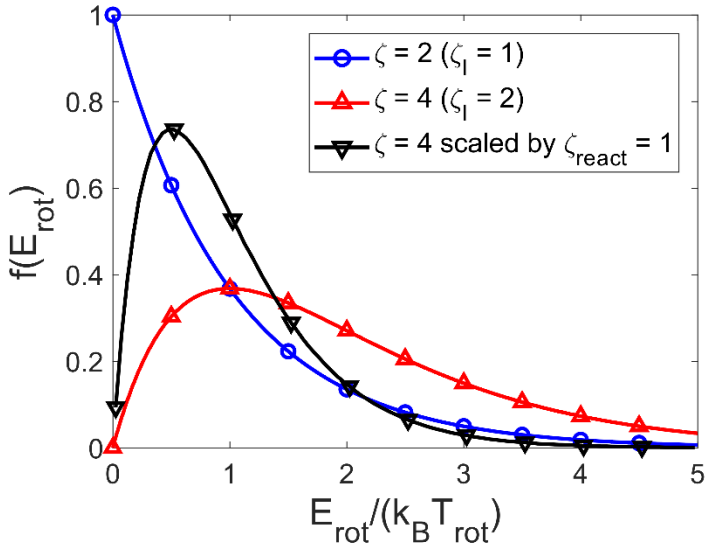

Figure 7.3 Analytic internal energy distribution functions for ζ = 2 and 4 and rDOF model distribution function scaled from ζ = 4 by a selected ζ_{react} value.

One final problem with of the TCE model remains to be discussed. The derivation of Eqn. 7.17 involved an integration over all collision energies, from the activation energy to infinity. In the past, most DSMC simulations assumed that the enthalpy of the reaction is equal to the activation energy of the forward rate, where the forward rate is defined as the endothermic side of the reaction. In turn, the activation energy for a backward reaction is then set to zero. These assumptions lead to errors in modeling the correct amount of energy absorbed or released in each reaction since the enthalpy of reaction is not typically equal to the activation energy. If the correct enthalpy of reaction is used, the TCE model may still encounter problems if this enthalpy is greater than the activation energy. Since a reaction cannot occur unless the collision energy is greater than both the enthalpy of reaction and the activation energy, the enthalpy of reaction is the minimum collision energy required in this case. Because Eqn. 7.17 was derived assuming

that any collision energy greater than the activation is allowed, collisions with energy between the activation energy and enthalpy of reaction values would result in a reaction probability of zero. This leads to an under-simulation of the reaction rate. While, in reality, this scenario is not physical as the activation energy must always be greater than or equal to the enthalpy of reaction, modifications of the Arrhenius rate for several reactions have violated this requirement in an attempt to fit rates that were previously incompatible with the TCE model.

7.3.5 Solutions for Satisfying Model Assumptions

While there are many underlying assumptions and restrictions, the TCE model is still applicable to many DSMC scenarios if the appropriate limitations are taken into account. Consider a standard chemically reactive DSMC simulation where rotational energy is modeled by a continuous distribution and vibrational energy is modeled by the discrete SHO. From the previously mentioned limitations, the vibrational energy model is not compatible with the TCE model. To appropriately address this issue and ensure that the correct Arrhenius rate is modeled, contributions from the vibrational modes of the colliding particles must be excluded from the calculation of Eqns. 7.15 and 7.16. The collision energy and contributing degrees of freedom, for this case, now depend solely on the rotational and relative translational values. The resulting collision energy is compared with the activation energy, then it and the contributing degrees of freedom values are used in Eqn. 7.17 to calculate the reaction probability. This means that the "total" collision energy used in the TCE model is no longer defined as the *total* energy of the colliding particles. Note, though, that now the collision energy calculated for the TCE model is no longer equal to the *total* energy that is used to determine the post-collisional states from the Borgnakke-Larsen model. Figure 7.2 demonstrates that the correct

reaction rate is simulated by DSMC when only the rotational mode is included to calculate the TCE probability. While this approach allows the TCE model to reproduce the correct Arrhenius rate, information from the vibrational modes no longer influences which particles react. It is not difficult to perceive situations where this result is troublesome as molecules in excited vibrational states will now react at the same rate as molecules in the vibrational ground state. With this in mind, it may be worthwhile in some cases, to purposely ignore the minor reaction rate error so that the vibrational modes contribute to determining which particles react. While it is likely that only slight errors in the reaction rate will be present for diatomic molecules simulated at high temperatures, problems may arise as the molecular complexity is increased. This approach cannot be extended to electronic excitation modeling since the observed errors are much greater for the much more widely spaced quantum electronic levels. The effects of including the electronically excited state energy in the TCE model can be seen for the O_2 dissociation reaction in Fig. 7.2. For this reaction, the rate is overpredicted by an even larger margin than the case with rotational and vibrational energy contributing to the TCE mode. On a large scale, it was found that the ionization rates were severely overpredicted when the electronic energy was included in the TCE model. It is likely that this problem resulted in an overprediction of ionization in the second nominal simulation and sensitivity analysis (Chapters 4 and 5).

7.4 Modeling Backward Reactions

If forward reactions are simulated by the TCE model, backward reactions must also be modeled in order to reproduce the equilibrium constant, K_{eq}, defined in Eqn. 7.5. Since DSMC simulations model chemical reactions on a per collision basis, the equilibrium constant cannot be directly calculated from Eqn. 7.6. Instead, the backward

reaction rate, k_b, must be represented by determining a reaction probability for each collision pair, similar to forward reactions. There are several current methods for calculating the backward reaction probability discussed in the following section. A new method developed in this dissertation is presented in Section 7.4.2.

7.4.1 Current Backward Reaction Models

The most common method for addressing backward reactions in DSMC is to reuse the TCE model, which requires that the backward reaction rate takes the Arrhenius form [3]. Since equilibrium constants, and not backward reaction rates, are published in most cases, the backward reaction rates must be fit to the Arrhenius form by rearranging Eqn. 7.5. As previously discussed in Section 7.3.4, the activation energy for backward reactions is typically set to zero when using the TCE model. This leaves only the pre-exponential constant, Λ_b, and the temperature exponent, η_b, to represent the backward reaction rate. Now both the forward and backward rate are represented by Arrhenius equations meaning that the equilibrium constant must also have this form. In actuality, the equilibrium constant typically has a more complex dependence on temperature than the Arrhenius form. To mitigate the errors caused by representing the equilibrium constant with an Arrhenius form, backward reaction rates are often strategically fit to the expected temperature range of the DSMC simulation. Even then, discrepancies in the reaction rate may still be evident and, in some cases, are egregious outside of the fit temperature range. The restrictions on the TCE model laid out in Section 7.3.2 must also be considered, increasing the difficulty in accurately matching the backward reaction rate to an Arrhenius form.

Due to the difficulties of simulating backward reactions with the TCE model, Boyd has proposed an improved approach to modeling these reactions [36][85]. Instead

of calculating a reaction probability based on the properties of each collision pair, a constant reaction probability in each DSMC cell is calculated for each reaction from the temperature of the cell. While this approach only allows for nonequilibrium to occur on the cell scale for backward reactions, this should have a negligible effect on the overall nonequilibrium of the simulation because backward reactions are relatively rare in the thermal nonequilibrium regions of typical DSMC applications. Boyd's method takes advantage of Eqns. 7.4-6 to determine the backward rate by assuming that the activation energy of the backward reaction is zero. The backward rate is then found to be

$$k_b(T) = \Lambda_f T^{\eta_f} \frac{\prod_i^{N_r} (Q_i)^{\alpha_i}}{\prod_j^{N_p} (Q_j)^{\beta_j}} V^{(\beta_p - \alpha_r)} \qquad \left[\frac{1}{s}\left(\frac{cm^3}{mol}\right)^{\beta_p}\right] \qquad [7.23]$$

where the reactant and products are defined from the forward direction (Eqn. 7.1). The reaction probability is then determined from the collision frequency, $\nu_{A,B}$, of the collision pair A and B as

$$P_{react} = \Lambda_f T^{\eta_f} \frac{\prod_i^{N_r} (Q_i)^{\alpha_i}}{\prod_j^{N_p} (Q_j)^{\beta_j}} V^{(\beta_p - \alpha_r)} \times \frac{n_B}{\nu_{A,B}} \qquad [7.24]$$

where n_B is the number density of the collision pair species used in the calculation of $\nu_{A,B}$. The temperature, T, and the total partition function, Q, for each species are calculated based on the cell temperature where the total partition function is determined from the translational, rotational, vibrational and electronic partition functions for that

particular species. If the reaction being considered is a recombination reaction, Eqn. 7.24 must also be multiplied by the number density of the third body.

In theory, this method should accurately represent the backward reaction rate and, therefore, reproduce the equilibrium constant. In practice, this is much more difficult than it seems. The calculation of the partition functions can become complex when a high degree of accuracy is desired. High order partition functions for each mode, coupling between rotation and vibration, temperature and density cut-offs for electronically excited levels, and a large number of input parameters all contribute to this complexity [75]. If low order partition functions are used, errors in the backward reaction rate may become an issue, especially at high temperatures. Also, additional parameters could be required even for these low order partition functions. Rotational, vibrational, or electronic partition function parameters may be essential to calculate an accurate total partition function for a species, regardless of whether those modes are included in the DSMC simulation. Even if low order partition functions are used, the partition functions for a species must be calculated in every cell where that species can potentially react. This process must be repeated at every timestep. For a large number of cells, the computational cost quickly increases, but has little benefit to the overall result since backward reactions are typically infrequent. In addition, the assumption that the backward reaction's activation energy is zero creates the same problems that the TCE model faces.

7.4.2 Improved Backward Reaction Model

To address the issue of accuracy, the following model for backward reactions simulated in DSMC is proposed. This model is similar to Boyd's method and is contained within the derivation of the backward reaction rate (Eqn. 27 in Ref. [85]). The proposed model calculates the backward reaction rate from Eqns. 7.4 and 7.5 as

$$k_b(T) = \frac{\Lambda_f T^{\eta_f} exp\left(-{E_{a_f}}/{k_B T}\right)}{K_{eq}(T)} \quad [7.25]$$

where T is calculated from the cell temperature and the backward reaction probability is then defined as

$$P_{react} = \frac{\Lambda_f T^{\eta_f} exp\left(-{E_{a_f}}/{k_B T}\right)}{K_{eq}(T)} \times \frac{n_B}{\nu_{A,B}} \quad [7.26]$$

where Eqn. 7.26 should be multiplied by the number density of the third body for a recombination reaction. Instead of calculating the equilibrium constant, K_{eq}, from partition functions, the equilibrium constant can be calculated from previously published curve fits. These published equations are fit to high order partition functions or ab initio calculations over a range of temperatures for each individual reaction and are generally considered accurate representations of the equilibrium constant. For example, if Park's equilibrium constant curve fit [47] is used, Eqn. 7.26 becomes

$$P_{react} = \frac{\Lambda_f T^{\eta_f} exp\left(-{E_{a_f}}/{k_B T}\right)}{\exp\left[\frac{A_1}{Z} + A_2 + A_3 \ln(Z) + A_4 Z + A_5 Z^2\right]} \times \frac{n_B}{\nu_{A,B}} \quad [7.27]$$

In Park's equilibrium constant equation, A_i are coefficients and $Z = 10{,}000/T$. Other than Park's curve fits, equilibrium constant values have been published in several sources with varying degrees of accuracy, including Gupta's curve fits [86] or the Gibbs free

energy approach applied in the NASA Chemical Equilibrium with Applications code [87].

Unlike the TCE model and Boyd's model, this approach does not require that the backward reaction rate's activation energy be equal to zero. Instead, the backward activation energy of a reaction, E_{a_b}, is defined as

$$E_{a_b} = E_{a_f} - \Delta H° \qquad [7.28]$$

where ΔH is the enthalpy of the forward reaction and E_{a_f} is the forward rate's activation energy. As DSMC is a particle method, this backward activation energy is important to calculate since the reaction is not allowed to occur for collisions that do not have enough energy. This means that Eqn. 7.26 is used when $E_c > max\left(E_{a_b}, -\Delta H°\right)$ and $P_{react} = 0$ otherwise. Care must also be taken so that the enthalpy removed from the system, when a reaction proceeds in one direction, is equivalent to the enthalpy added to the system when the reaction happens in the opposite direction. For example, energy is removed from the total collision energy for an endothermic dissociation reaction, but when the corresponding recombination reaction occurs, the same amount of energy is added to the total collision energy.

Eqn. 7.26 is actually a special case that assumes $E_{a_b} \ll k_B T$ which is typically a valid assumption for most reactions in DSMC simulations. If the backward reaction's activation energy is significant or the simulated temperature is low enough, a correction term must be included. This correction term is derived by starting from Eqn. 7.13 and considering the collision energy, E_c [3]. When the VHS model is used, the distribution integrated over all collision energy values, normalized to $k_B T$ is

$$f\left(\frac{E_c}{k_B T}\right) = \frac{1}{\Gamma\left(\zeta_I + \frac{5}{2} - \omega_{A,B}\right)}\left(\frac{E_c}{k_B T}\right)^{\zeta_I + \frac{3}{2} - \omega_{A,B}} exp\left(-\frac{E_c}{k_B T}\right) \quad [7.29]$$

where ζ_I is determined from Eqn. 7.15. By integrating from E_{a_b} to infinity, the fraction of collisions with $E_c > E_{a_b}$ is found to be

$$\frac{dN}{N} = \frac{\Gamma\left(\zeta_I + \frac{5}{2} - \omega_{A,B}, E_{a_b}/k_B T\right)}{\Gamma\left(\zeta_I + \frac{5}{2} - \omega_{A,B}\right)} \quad [7.30]$$

with the numerator defined as an incomplete gamma function. When $E_{a_b} \ll k_B T$, Eqn. 7.30 approaches one and can be ignored, but otherwise, this ratio must be calculated directly and applied to the reaction probability by dividing Eqn. 7.26 by Eqn. 7.30. A simplification of Eqn. 7.30 can be made when $E_{a_b} \gg (\zeta_I + 3/2 - \omega_{A,B}) k_B T$, but this is generally not the case for backward reactions [75]. Note that, like the TCE model, the degrees of freedom used to calculate Eqn. 7.30 must correspond to the energy modes that contributed to determining if $E_c > E_{a_b}$. In addition, for the rare case where $-\Delta H° > E_{a_b}$, the backward activation energy in Eqn. 7.30 should be replaced by $-\Delta H°$ since the minimum collision energy for a reaction to be possible is now defined by the enthalpy of reaction. Finally, this correction should not be applied when $max\left(E_{a_b}, -\Delta H°\right) < 0$ as the correction factor will result in unintended modifications of the reaction rate.

The approach developed for the proposed backward reaction model can also be adopted to improve Boyd's model. While the original derivation of Boyd's model assumed that the enthalpy of reaction is equal to the forward activation energy, this simplification is not necessary. Instead, the exponential terms from the Arrhenius forward rate (Eqn. 7.4) and the equilibrium constant (Eqn. 7.6) should not cancel and should

appear in Eqns. 7.23 and 7.24. Since it is now possible for the backward activation energy to be nonzero, the correction factor in Eqn. 7.30 should also be applied where necessary. Finally, it must be noted that neither Boyd's or the proposed model guarantee that the reaction probability will be less than one. While probabilities greater than one will result in errors modeling the backward reaction rate, it is unlikely that these errors negatively affect the simulation results. Since both models rely on cell temperature, it is reasonable to expect that the mixture has been fully reacted before the cell temperature corresponding to a probability of one is reached. On the other hand, probabilities greater than one resulting from the TCE model are possible at much lower temperatures due to the reliance on collision energy to calculate the probability.

7.5 Backward Reaction Model Comparisons

7.5.1 Reaction Rate Comparison

With the introduction of a new backward reaction model, several assessments of its relationship to the old models must be completed. Figure 7.4 compares the backward reaction rate for the Zeldovich reaction, $O + N_2 \rightleftharpoons N + NO$, calculated from each of the three models to the exact backward reaction rate. The backward rate for each model is determined from a DSMC simulation following the same method applied in Section 7.3. Here, the "exact" backward rate is considered to be the ratio of the forward rate over the equilibrium constant curve fit, both determined by Park [47]. The equilibrium constant is determined from detailed calculations of the partition functions and curve fit over some temperature range. The equilibrium constant, and therefore the backward reaction rate, is only considered accurate within this temperature range. Park's equilibrium constant was curve fit with five temperature points between 2,000 and 10,000 K. Although Park states that the fit diverges only slightly at high temperatures [47], Gupta has shown these errors

can be large for some reactions [86]. The parameters used to calculate the forward rate and equilibrium constant are listed in Table 7.1. Since the equilibrium constant is a function of density at high temperature due to temperature cutoffs for the atomic electronic partition functions, the current equilibrium constant is selected to correspond to the number density of the scenarios modeled [86].

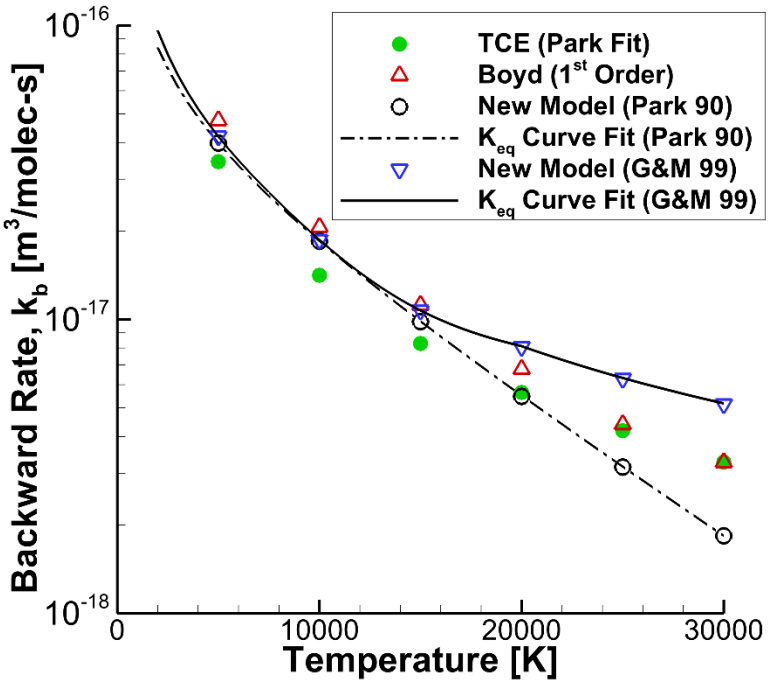

Figure 7.4 Comparison of the exact backward reaction rate for $O + N_2 \rightleftharpoons O + NO$ with DSMC using the TCE model, Boyd's model, and the proposed model.

First, the TCE model using a backward rate in Arrhenius form (Table 7.1), specifically fit to Park's parameters, is compared with the exact rate [88]. The Arrhenius form for the TCE reaction rate was fit to the temperature range between 10,000 and 20,000 K but is intended to reproduce the entirety of Park's curve fit. Even within this range, the TCE model displays noticeable error and above 20,000 K the error grows

dramatically with increasing temperature. This degree of error is expected since the Arrhenius equation cannot appropriately reproduce the complex dependence of the equilibrium constant on temperature and the Arrhenius parameters are constrained by the TCE model. Figure 7.4 also compares Boyd's approach (Eqn. 7.24) using first order partition functions with the exact rate. The exact partition function for translational, rigid rotor for rotational, SHO for vibrational, and quantum electronic partition functions are used here [85]. In order to reproduce Park's equilibrium constant, parameters for the partition functions were obtained from Refs. [85] and [47] (Table 7.2). Even when using Park's parameters, Fig. 7.4 shows that minor errors are evident below 20,000 K. It must be noted that above 20,000 K, Boyd's model is not expected to match with Park's. In this region, it is likely that Boyd's model is more accurate, but without calculating high order partition functions, a conclusion about the accuracy in this temperature range cannot be made. Finally, the backward reaction rate calculated by the proposed model is compared to the exact rate by directly using Park's equilibrium constant (Eqn. 7.27). As shown in Fig. 7.4, the simulated backward rate reproduces the exact backward rate identically for the entire temperature range.

A second test of the proposed model was conducted for the backward reaction rate calculated from the equilibrium constant curve fit determined by Gordon and McBride (G&M) [87]. The work published by G&M provides a large set of piecewise curve fits between 200 and 20,000 K where each equilibrium constant is fit using the enthalpy and entropy of the participating species. The advantage of using the G&M equilibrium constants is that they are commonly used in computational fluid dynamics (CFD) simulations. In addition, the curve fits are easily applied by following the approach detailed in Ref. [89] and using the curve fit and enthalpy data available in the *thermo.inp* file located in the NASA Chemical Equilibrium with Applications (CEA)

code [90]. Unfortunately, these curve fits are difficult to extrapolate because they tend to become unstable. For example, the G&M curve fit for the $O + N_2 \rightleftharpoons O + NO$ reaction is shown in Fig. 7.5. Above 20,000 K, the equilibrium constant quickly trends towards zero. This leads to unphysical results when the G&M equilibrium constant is used in Eqn. 7.26 as a large backward reaction probability is calculated, resulting in unexpected backward reactions at temperatures above 20,000 K. Typically, CFD simulations set the backward reaction rate to zero outside of the G&M curve fit's valid range. For CFD this is a reasonable strategy, but fluctuations in the DSMC cell temperature make this occurrence more likely. As an alternative to setting the backward reaction probability to zero, a reasonable extrapolation of the G&M equilibrium constant can be performed. As the equilibrium constant is approximately linear on a semi-log plot vs $1/T$, a least squares regression fit can be performed on the G&M equilibrium constant at high temperatures (Fig. 7.5). A continuous extrapolation of the equilibrium constant is obtained by shifting this least squares fit so that the extrapolation begins at the highest valid temperature of the G&M curve. An example of the G&M fit combined with the extrapolation is demonstrated in Fig. 7.5. This equilibrium constant was used to determine the G&M backward reaction rate shown in Fig. 7.4. The same equilibrium constant was then applied with the proposed backward reaction model. As seen in Fig. 7.4, the proposed model again reproduces the backward reaction rate exactly. The same extrapolation method could be applied to the lower bound of the G&M curve fit, but it may be more accurate to use Boyd's model and calculate the partition functions directly at these low temperatures, instead of using a least squares approximation, since low order partition functions should be sufficient. In the scenarios modeled in this dissertation, calculation of the lower G&M temperature bound is not an issue as temperatures this low will not be experienced.

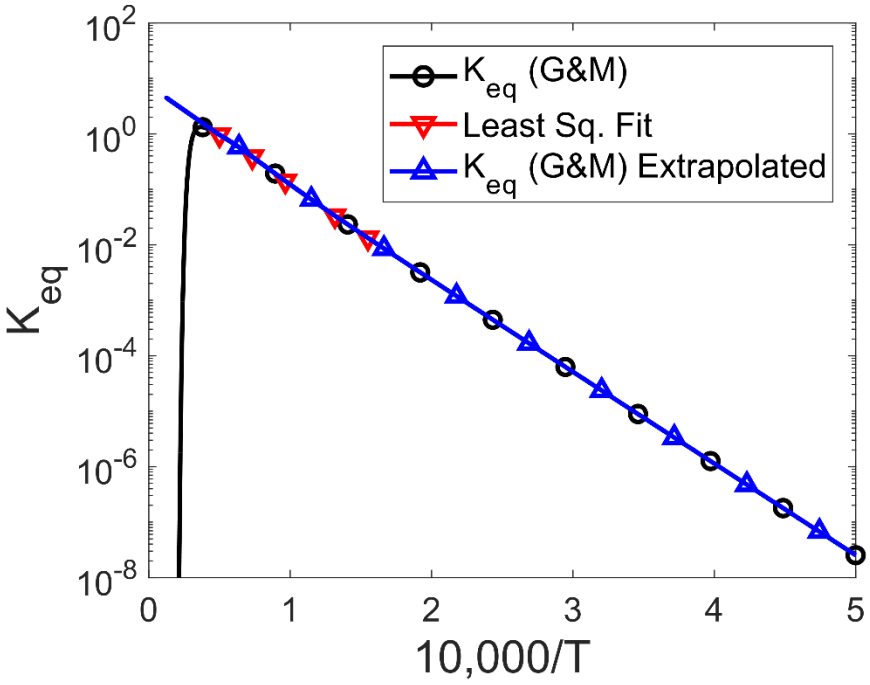

Figure 7.5 Analysis of the Gordon and McBride (G&M) equilibrium constant as a function of temperature.

7.5.2 1-Dimensional Shock Comparison

To demonstrate the importance of modeling backward reaction rates correctly in an ionizing, hypersonic shock, each of the models is used to simulate the EAST experiment examined in Chapter 4. This scenario reproduces the conditions of a lunar return trajectory at 10.26 km/s and pressure of 0.2 Torr using a synthetic air mixture of 79% N_2 and 21% O_2. The CHIPS code was used to simulate these conditions three separate times, applying the TCE model, Boyd's model with first order partition functions, and the proposed model for simulating backward reactions. The same parameters as in the previous CHIPS simulations were used for the forward reaction rates

and for the backward rates if the TCE model is used (Tables 3.2, 3.4, and 3.5). The proposed model calculates the backward reactions from the Gordon and McBride equilibrium constants and uses the high temperature extrapolation described in the previous section [87]. The results of comparing these models are plotted in Fig. 7.6a-c. It also should be noted that the TCE model was used to simulate forward reactions and the rotational and vibrational modes were included in the TCE total collision energy, even though a discrete vibrational distribution is used. As mentioned in Section 7.3.4, the inclusion of discrete vibrational energy in the TCE calculations should not lead to significant errors in this case because the temperatures modeled are typically higher than the characteristic vibrational temperatures of 11-species air molecules and the molecules involved in this mixture are diatomic. However, in this iteration of the EAST scenario simulation, the electronic energy is not allowed to contribute to the forward reaction rate, unlike previous simulations completed in Chapters 4 and 5. This is due to the significantly discrete nature of electronic excitation. Removing electronic excitation from consideration has a noticeable effect when comparing Fig. 7.6a-c with Fig. 4.5a-c, resulting in a perceptible increase in the temperatures and decrease in the ionized particle number densities.

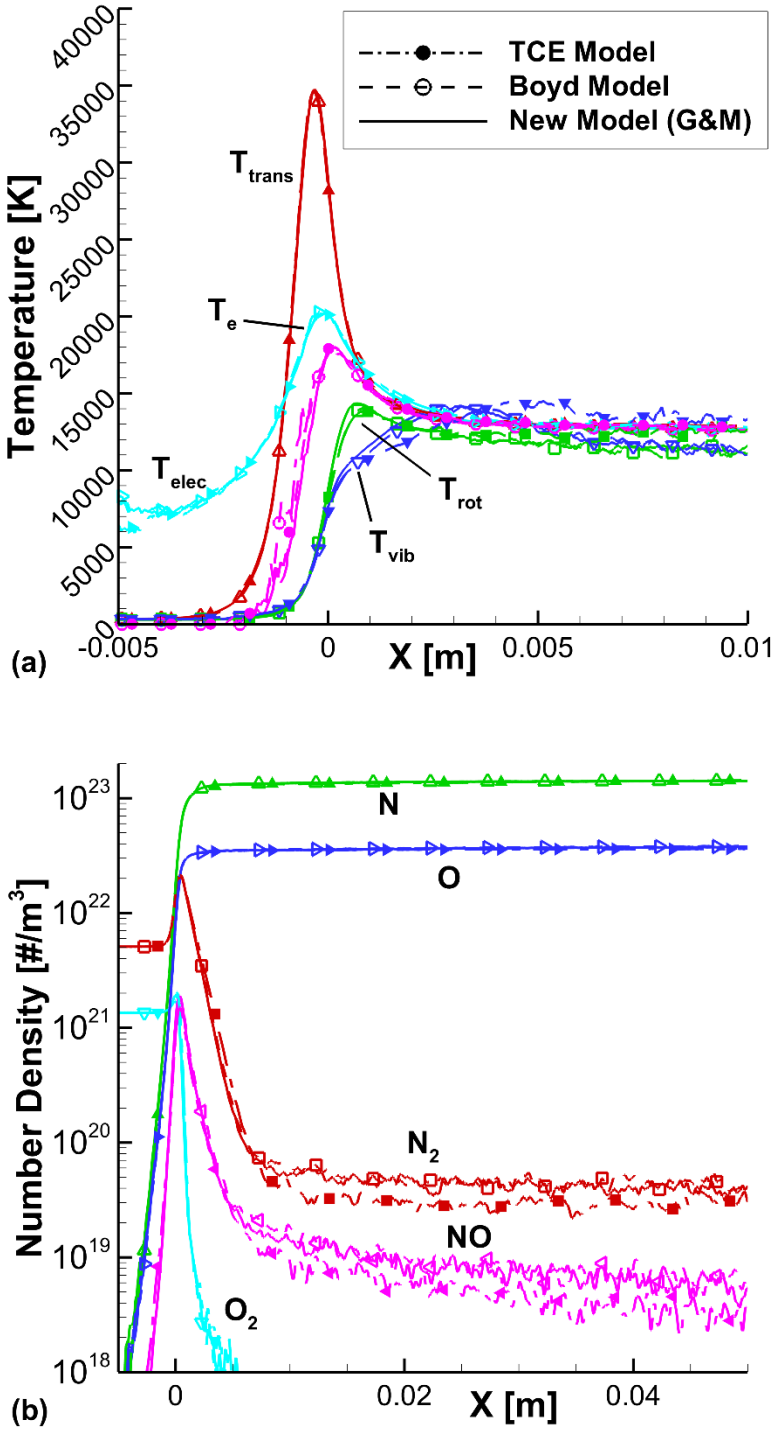
TCE Model
Boyd Model
New Model (G&M)
Temperature [K]
40000
35000
30000
25000
20000
15000
10000
5000
0
T_trans
T_e
T_elec
T_rot
T_vib
-0.005
0
X [m]
0.005
0.01
(a)
Number Density [#/m^3]
10^23
10^22
10^21
10^20
10^19
10^18
N
O
N_2
NO
O_2
0
0.02
X [m]
0.04
(b)

Figure 7.6

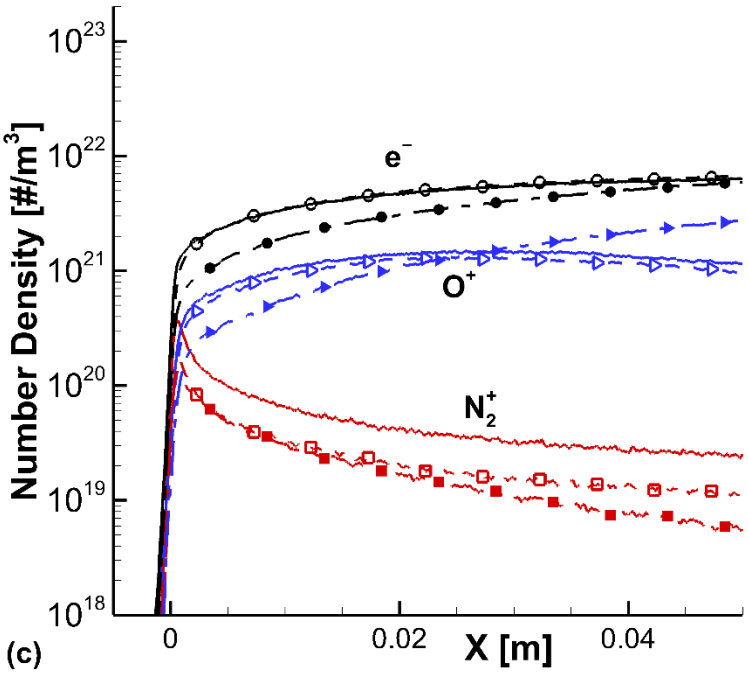

Figure 7.6 Comparison of the TCE (dash-dotted line, solid symbols), Boyd's (dashed line, open symbols), and the proposed (solid line) models for CHIPS simulations of EAST Shot 37. *(a) Bulk temperatures. (b) Neutral particle number densities. (c) Charged particle number densities.*

When comparing the results from using the different backward reaction models, several discrepancies can be identified. In Fig. 7.6a, the simulated temperatures from the three models agree well, except for the vibrational temperature. The TCE model predicts a slightly higher vibrational temperature downstream of the shock than the other two models, which are in good agreement with each other. This is likely due to the TCE model reproducing an incorrect recombination rate which leads to the slight underprediction of N_2 and O_2 as seen in Fig. 7.6b. Again, the proposed model and Boyd's model are in relatively good agreement for all the neutral particle number densities. The charged particle number densities are compared in Fig. 7.6c where the number densities of N^+, O_2^+, and NO^+ are removed for clarity. This figure demonstrates substantial

disagreement between the models, especially for the TCE model. When using the TCE model, the number density of O^+ is continuously increasing downstream of the shock while O^+ increases initially and then decreases further downstream when using Boyd's or the proposed model. This occurs because Arrhenius form reaction rates are not available in the current literature for O^+ electron capture reactions. In fact, several electron capture and reverse charge exchange reactions are missing from the TCE reaction set (Table 3.5). These reactions could be fit to an Arrhenius form, but this attempt is likely to be a wasted effort because of the difficulty in fitting charged reactions to an Arrhenius form within the TCE model's constraints. Both the proposed model and Boyd's model produce similar charged particle number densities, with the exception of N_2^+. This difference is likely a result of using first order partition functions in Boyd's model. As the complexity of the colliding particles increases, this simplification will result in greater error.

While the discrepancies between predictions from the three backward reaction models does not seem to be extreme for an ionizing, hypersonic shock case, this would not be true in every instance. For example, if a cold entry vehicle body were place behind the shock, it would force the temperature to equilibrate quickly to some low temperature value. This equilibration would require a much larger number of backward reactions, especially electron capture reactions. In this case, the chosen backward reaction model would have a greater influence on the results.

7.5.3 Model Analysis

These comparisons demonstrate several advantages of using the equilibrium constant curve fits instead of low order partition functions, but also raises some important items to consider. The proposed method can only simulate the backward reaction rate with the same accuracy of the equilibrium constant used in Eqn. 7.26. Care must be taken

to use equilibrium constants that are valid in the expected temperature range. If large errors in the equilibrium constant are anticipated for the simulated temperatures, Boyd's model may be more appropriate. However, this should not typically detract from the use of the proposed model because high accuracy equilibrium constants are easily obtained for most temperature ranges of interest. If equilibrium constants for a specific reaction are completely unavailable, Boyd's model is necessary. Another consideration is that these three models have differing requirements for compiling rates from different sources. The forward and backward reactions rates used in the TCE model *must* correspond to each other since the backward rate is curve fit to the forward rate and a specific equilibrium constant. For both the TCE and proposed models, the forward rate and equilibrium constant should be a matching pair. Compiling the forward rate and equilibrium constant from separate sources risks errors in the backward rate since the activation energy should be identical for both equations. While this is a requirement, activation energy values are relatively well known and should deviate only slightly between different sources, meaning that mixing forward rates and equilibrium constants from different sources should not typically result in large errors. Boyd's model has an advantage in this regard since only the forward rate is required.

When considering computational cost, both the proposed method and Boyd's model using low order partition functions provide significant improvement compared to the TCE model, resulting in a 1.8x speedup of a 0-dimensional relaxation simulation with similar results for other DSMC simulations. The efficiency of the proposed method and Boyd's model have comparable computational cost depending on the order of the partition functions used in Boyd's method. Conclusions on the overall computational efficiency for a full DSMC simulation of a reacting mixture are not as clear when comparing the two models. The required number of calculations per cell scales with the

number of reactions for the proposed method, whereas the number of calculations per cell scales with the number of simulated species for Boyd's model. Implementations of both Boyd's and the proposed methods could potentially increase computational efficiency from look-up tables or parametric curve fits calculated on the fly since the rate of each reaction is only a function of cell temperature.

The greatest advantage for the proposed method is that, while it is new for DSMC, this method is a standard approach used in continuum modeling and can make use of the same equilibrium curve fits. In addition, Gordon and McBride have published a large database of parameters required to calculate the equilibrium constant that is readily available [87]. Since this database is commonly used in CFD, the proposed backward reaction method reduces the number of discrepancies encountered when attempting to match with continuum simulations or to interface between the continuum and rarefied regimes.